Received: 15 March 2024 | Revised: 11 July 2024 | Accepted: 29 July 2024

DOI: 10.1111/gcb.17474

Global Change Biology WILEY

RESEARCH ARTICLE

Asymmetric effects of hydroclimate extremes on eastern US tree growth: Implications on current demographic shifts and climate variability

Justin T. Maxwell[1] | Tsun Fung Au[2,3] | Steven A. Kannenberg[4] | Grant L. Harley[5] | Matthew P. Dannenberg[6] | Darren L. Ficklin[1] | Scott M. Robeson[1] | Macarena Férriz[1] | Michael C. Benson[7] | Benjamin R. Lockwood[8] | Kimberly A. Novick[9] | Richard P. Phillips[10] | Maegen L. Rochner[11] | Neil Pederson[12]

[1]Department of Geography, Indiana University, Bloomington, Indiana, USA

[2]Institute for Global Change Biology, University of Michigan, Ann Arbor, Michigan, USA

[3]Department of Ecology and Evolutionary Biology, University of Michigan, Ann Arbor, Michigan, USA

[4]Department of Biology, West Virginia University, Morgantown, West Virginia, USA

[5]Department of Earth and Spatial Sciences, University of Idaho, Moscow, Idaho, USA

[6]Department of Geographical and Sustainability Sciences, University of Iowa, Iowa City, Iowa, USA

[7]School of Integrative Biology, University of Illinois, Urbana-Champaign, Illinois, USA

[8]Department of Ecosystem Science and Management, Pennsylvania State University, State College, Pennsylvania, USA

[9]O'Neil School of Public and Environmental Affairs, Indiana University, Bloomington, Indiana, USA

[10]Department of Biology, Indiana University, Bloomington, Indiana, USA

[11]Department of Geographic and Environmental Sciences, University of Louisville, Louisville, Kentucky, USA

[12]Harvard Forest, Harvard University, Petersham, Massachusetts, USA

Correspondence
Justin T. Maxwell, Department of Geography, Indiana University, Bloomington, IN, USA.
Email: maxweljt@indiana.edu

Funding information
Harvard Forest Bullard Fellowship, Harvard University; Indiana University Vice Provost for Research Faculty Research Program Bloomington; Division of Atmospheric and Geospace Sciences, Grant/Award Number: 1805276 and 1805617; National Institute of Food and Agriculture, Grant/Award Number: 2017-67013-26191

Abstract

Forests around the world are experiencing changes due to climate variability and human land use. How these changes interact and influence the vulnerability of forests are not well understood. In the eastern United States, well-documented anthropogenic disturbances and land-use decisions, such as logging and fire suppression, have influenced forest species assemblages, leading to a demographic shift from forests dominated by xeric species to those dominated by mesic species. Contemporarily, the climate has changed and is expected to continue to warm and produce higher evaporative demand, imposing stronger drought stress on forest communities. Here, we use an extensive network of tree-ring records from common hardwood species across ~100 sites and ~1300 trees in the eastern United States to examine the magnitude of growth response to both wet and dry climate extremes. We find that growth reductions during drought exceed the positive growth response to pluvials. Mesic species such as *Liriodendron tulipifera* and *Acer saccharum*, which are becoming more dominant, are more sensitive to drought than more xeric species, such as oaks (*Quercus*)

and hickory (*Carya*), especially at moderate and extreme drought intensities. Although more extreme droughts produce a larger annual growth reduction, mild droughts resulted in the largest cumulative growth decreases due to their higher frequency. When using global climate model projections, all scenarios show drought frequency increasing substantially (3–9 times more likely) by 2100. Thus, the ongoing demographic shift toward more mesic species in the eastern United States combined with drier conditions results in larger drought-induced growth declines, suggesting that drought will have an even larger impact on aboveground carbon uptake in the future in the eastern United States.

KEYWORDS
climate change, demographic shift, drought, pluvial, tree rings

1 | INTRODUCTION

Globally, forests are vulnerable to changes in climatic conditions (Allen et al., 2010; Breshears et al., 2005; McDowell et al., 2008) and from human land-use decisions (Hamrick, 2004; McDowell et al., 2020). Forests in the eastern United States are a classic example, with well-documented, frequent, and extensive anthropogenic and natural disturbances over the past ca. 200 years. Forest species composition across the eastern United States have been strongly influenced by human land management, where frequent fire and thinning before the 1850s by Indigenous groups prompted forests dominated by *Quercus* (oak) and *Carya* (hickory). European colonization was followed by massive deforestation and later reforestation (along with regeneration) coupled with fire suppression. Such practice resulted in a decline in the prevalence of *Quercus* and *Carya* species and allowed the establishment of other less fire-tolerant species such as *Acer* spp. (maple), *Fagus grandifolia* (American beech), and *Liriodendron tulipifera* (tuliptree) (Fei et al., 2011), which are now poised to replace the aging oaks and hickories that have lower regeneration rates (Novick et al., 2022).

The climate in the eastern United States is also changing. Over the last several decades, an extended wet period (or pluvial) has been prevalent across large parts of the eastern United States (Ford, 2014; Karl et al., 1996; Maxwell et al., 2016; Maxwell & Harley, 2017; Pederson et al., 2013). Furthermore, the rate of temperature increase in the eastern United States compared to other regions of the world has been muted, largely due to reforestation (Barnes et al., 2024), increased aerosols (Mascioli et al., 2017; Yu et al., 2014) and interactions between temperature and changing precipitation regimes (Eischeid et al., 2023). Thus, the wetter and relatively cooler climate has reinforced and accelerated ongoing demographic shifts in eastern United States forests, resulting in less drought and fire (McEwan et al., 2011). In the future, the rate of reforestation is likely to decrease, diminishing the temperature buffering effect (Barnes et al., 2024), likely leading to hotter and drier conditions. Combined with the continued warming of global temperatures from anthropogenic emissions, hotter and drier conditions in the eastern United States are likely to accelerate (Ficklin & Novick, 2017; Wehner et al., 2017), potentially leading to climate having a larger role on forest species composition.

The likelihood of a shift from an exceptionally wet climate to a more arid climate in eastern North America requires an understanding of the response of species and forest stands to climatic extremes (Costanza et al., 2023). The impact of climatic extremes on tree growth depends on the timing, context, duration, and intensity of water stress (Schwarz et al., 2020), with trees experiencing greater growth reductions when drought occurs during the growing season (Delpierre et al., 2016; D'Orangeville et al., 2018; Hoffmann et al., 2018). Additionally, forest composition may play a role in drought response since tree species diversity may buffer the sensitivity of forests to climate extremes (Anderegg et al., 2018; Grossiord et al., 2020; Isbell et al., 2015). Less is known about forest responses to pluvial conditions (but see Jiang et al., 2019; Lockwood et al., 2023). Thus, characterizing the response of different species assemblages to climatic extremes is crucial for understanding forest dynamics and productivity under projected future scenarios. This understanding is especially important in the eastern United States, where forests have historically sequestered ca. 40% of regional carbon emissions (Pan et al., 2011). The future fate of this sink is uncertain and hinges on tree- and stand-level responses to climate extremes.

While ecophysiological responses to droughts and pluvials, such as changes in gas exchange, are useful for examining species-specific responses, the short length of such records limits the number of extremes to examine species-specific responses. Using tree rings from mature, canopy-dominant trees extends the number of extreme wet and dry events that we can examine to see how growth responds to extreme climatic conditions. Furthermore, growth is often decoupled from photosynthesis (Cabon et al., 2022; Dow et al., 2022), and this is exacerbated during drought (Kannenberg et al., 2022). Thus, examining growth directly can give insight into how droughts will impact long-term carbon storage in woody biomass and how ongoing demographic shifts could impact the forest response to future climate change in the eastern United States.

Here, we examine the magnitude of growth responses of several common eastern US hardwood tree species to both wet and dry climate extremes. We hypothesize that ongoing demographic shifts are producing forests that are more susceptible to deleterious drought impacts on growth, a change with negative impacts to carbon sequestration. We further examine if increased growth sensitivity to pluvial conditions can offset growth losses to drought. To test the hypothesis, we leverage a broad and diverse network of ~100 tree-ring chronologies (~1300 trees), focusing on five of the most widespread species throughout the eastern United States. We further examine how this demographic shift will impact future responses of eastern US forests by using climate model projections for a number of greenhouse gas scenarios.

2 | METHODS

2.1 | Study region/samples

The study region encompasses a large portion of the Eastern Deciduous Forest biome in North America (Figure 1). The climate over this area is humid continental with the southern portion of the study region having a humid subtropical climate. We targeted canopy-dominant trees from some of the most common species in this region, species that also employ a range of water-use strategies from aggressive (i.e., anisohydric; *Quercus rubra and Quercus alba*), intermediate (*Carya ovata* and *Acer saccharum*), and conservative (i.e., isohydric; *L. tulipifera*) (Novick et al., 2022; Roman et al., 2015; Yi et al., 2019).

2.2 | Tree-ring processing

We gathered tree-ring chronologies (published in: Maxwell et al., 2019, 2020, 2022; Pederson, 2005) and collected samples from three new sites resulting in chronologies across 36 forest stands for a total of 99 chronologies. All 36 sites had at least two co-occurring species, while 19 sites had three, and six sites had four or more. While each of the five species were not present at every site, sampling those that are growing in the same landscape position at each site decreases the confounding influence of site conditions and allows for a clearer comparison of species-specific growth response to extreme climate (Au et al., 2020; Au & Maxwell, 2022; Lockwood et al., 2023). Overall, we gathered a total of 18 chronologies for *Q. rubra*, 25 for *Q. alba*, 19 for *C. ovata*, 15 for *A. saccharum* and 22 for *L. tulipifera* across the eastern deciduous forest (Figure 1).

The gathered published and newly collected species-specific chronologies were generated from 5 to 50 trees, giving us a total of 1299 trees used in this study. We followed the same methods that were used for the published chronologies to collect tree-ring data at the three new sites, which were standard collection methods for dendrochronological studies. Thus, we targeted canopy-dominant trees and extracted two core samples per tree. The ring widths were

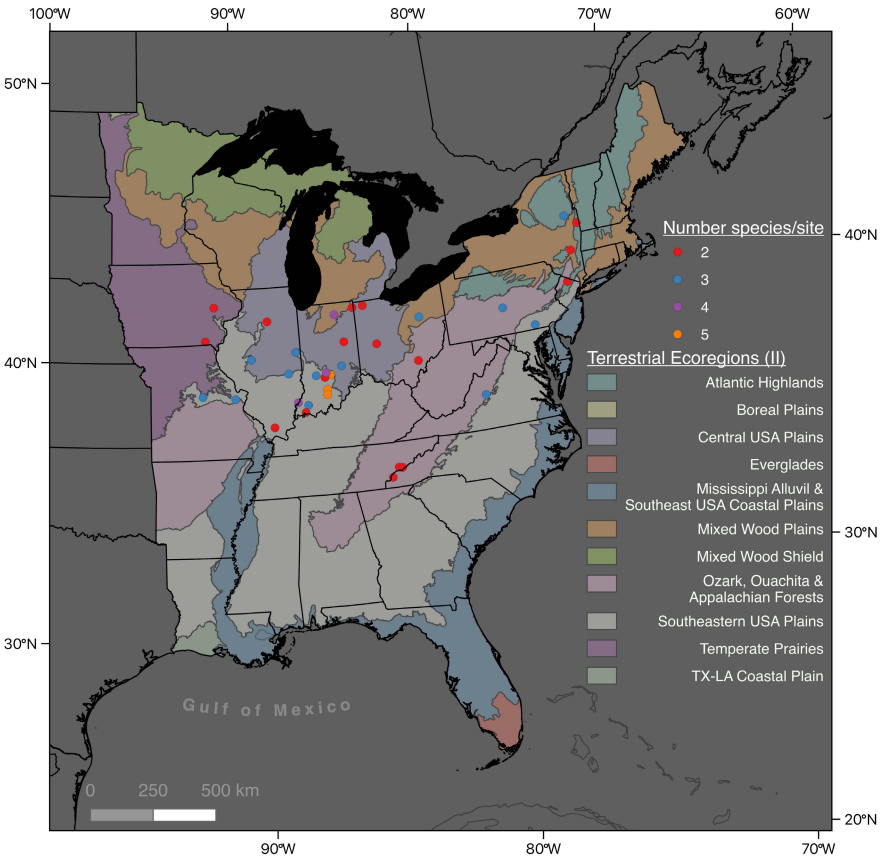

FIGURE 1 Tree-ring study sites across the Eastern Deciduous Forest biome. Map of tree-ring sites showing the number of species-specific chronologies per study site along with the level two terrestrial ecoregions as defined by Commission for Environmental Cooperation (http://www.cec.org/north-american-environmental-atlas/).

visually crossdated using the program COFECHA (Holmes, 1983) to statistically ensure accurate dating. All chronologies had high interseries correlations, ranging from $r = .51$ to .72 ($p < .01$). After gathering the published chronologies, we reduced growth related to non-climatic influences, including biological growth trends by standardizing each measurement series with a two-third spline (Cook & Peters, 1981) and adjusting for endpoints (Bussberg et al., 2020) using the program ARSTAN (Cook, 1985).

Sampling from canopy-dominant trees while not including information from the subcanopy can introduce a bias when examining species-specific responses to climate (Dye et al., 2016). Traditionally, canopy-dominant species were thought to be more sensitive to climate (Alexander et al., 2018) compared to subcanopy trees, but this may not be the case in more mesic forests, such as in the eastern United States, where the subcanopy trees could have a larger decrease in growth during hot periods (Rollinson et al., 2021). However, canopy-dominant trees sequester carbon for longer periods, account for more biomass and carbon reserve (Bennett et al., 2017), and have lived long enough to experience multiple droughts and pluvials of differing intensities. Thus, they are arguably a fundamental portion of the forest canopy for understanding impacts on growth from climate extremes and their consequences for carbon sequestration.

2.3 | Climate data

We gathered monthly standardized precipitation-evapotranspiration index (SPEI; Beguería et al., 2014) data for the nearest (0.5°) grid point to each forest stand. The SPEI is standardized based on a probabilistic mapping of the precipitation (water supply) minus potential evapotranspiration (water demand) distribution onto a standard normal distribution, producing an index where 0 represents median conditions for a given location over the time period used for the fitting. This approach allows us to compare the influence of mild, moderate, and extreme dryness and wetness on tree growth across multiple sites that experience different climatic regimes. Because both water supply and water demand can influence tree growth, incorporating an index that includes both metrics is important (Novick et al., 2024; Williams et al., 2013). The SPEI is multiscalar, so it also allows us to evaluate how the duration of abnormal to extreme wet and dry conditions impact species-specific growth. We gathered SPEI for three temporal scales (1, 3, and 6 months; hereafter SPEI1, SPEI3, and SPEI6) to represent short term to growing season length anomalies in soil moisture. To capture climatic conditions that could influence the entire growing season, we examined conditions from March to August, using SPEI6 for August. To represent the peak of the growing season, we examined SPEI3 in July, which represents conditions from May to July. Lastly, for the short timescale (SPEI1), we gathered data for each month from May to August, which are the most important months for growth in eastern North America (D'Orangeville et al., 2018). We present the results from SPEI6 in the main text and provide the shorter timescale results, which all were similar to those from SPEI6, in the supplemental materials.

2.4 | Drought and pluvial effects

To determine how mild to extreme departures in water supply and demand impact species-specific growth, we calculated drought and pluvial effects for each species. We defined three, mutually exclusive drought thresholds, from mild (SPEI ±1.0, which probabilistically equates to one standard deviation from the mean) to moderate (SPEI ±1.5) and extreme (SPEI ±2.0). For each threshold, we calculated the percentage growth change during a drought or pluvial (i.e., drought and pluvial effects) by averaging the standardized ring width (SRW) for all years that were classified as a drought (SRW_d) or pluvial (SRW_p). We then calculated the averaged ring width for non-drought and non-pluvial years (SRW_n). Drought effects were calculated as the difference between the averaged SRW during drought from the normal years then divided by averaged growth during normal years and multiplied by 100 to get a percentage change (Au et al., 2020; Kannenberg et al., 2019). Pluvial effects were calculated in the same manner except with the difference between the averaged growth during pluvial years and normal years.

$$\text{Drought effect} = \frac{SRW_d - SRW_n}{SRW_n} \times 100$$

where SRW_d and SRW_n are the average standardized growth for all drought years and normal years, respectively.

$$\text{Pluvial effect} = \frac{SRW_p - SRW_n}{SRW_n} \times 100$$

where SRW_p and SRW_n are the average standardized growth for all pluvial years and normal years, respectively.

We calculated drought and pluvial effects for each month from May–August for SPEI1, May–July average for SPEI3, and March–August average for SPEI6. To determine if the mean effects were significantly different across the species, we used one-way ANOVA with a Tukey HSD post hoc test.

To examine the lasting effects of extreme wet and dry conditions on SRW, we calculated the growth differential percentage (Lloret et al., 2011) where we formed the ratio of the mean SRW during the 2 years following the extreme year (Kannenberg et al., 2019) subtracted from the growth during the extreme year in the numerator and the mean of SRW during the 5 years preceding the extreme year (Au et al., 2022) in the denominator:

$$\text{Growth differential} = \frac{SRW_{post1-2} - SRW_e}{SRW_{pre1-5}} \times 100$$

where e represents the year of an extreme event.

We excluded extreme years that occurred within 5 years following or 2 years prior to another event. We chose to examine only the 2 years following an extreme event since previous research has found that legacies longer than 2 years are relatively rare in Eastern Deciduous Forests (Kannenberg et al., 2019). When examining the growth differential percentage from pluvials, the resulting index typically will be negative, while recovering from droughts will result in a positive growth differential percentage. In addition to drought

and pluvial effect size, we compared the overall response to climate for each species (i.e., between the SRW and SPEI during the period of overlap, 1901–2015) using both a linear and a quadratic regression model. We then used both the Akaike information criterion (AIC) and adjusted R^2 to evaluate model performance and fit, finding AIC to be lower and adjusted R^2 to be higher for the quadratic model for all species (Table S1).

2.5 | Scaling for forest response

To examine how our results using 36 forest stands may scale to larger spatial scales, we used a community-weighted mean approach based on composition estimates of the canopy from the Forest Inventory and Analysis (FIA) for the study region. Because our study sites cover a large area and species composition varies dramatically over space, we calculated multiple forest response scenarios based on species compositions found throughout the eastern United States including: (1) a xeric species (*Quercus* and *Carya*) dominated forest with *Quercus* making up 40%, *Carya* 40%, *Acer* 10%, and *Liriodendron* 10%; (2) a mesic species dominated forest where *Acer* makes up 40%, *Liriodendron* 40%, *Quercus* 10%, and *Carya* 10%; and (3) a mixed forest, where *Quercus*, *Carya*, *Liriodendron*, and *Acer* each makes up 25% of the forest. In the FIA data, we did not see an *Acer* or *Liriodendron* dominated forest and thus did not create one for this analysis. Similarly, there were other assemblages like "beech-maple" (*Fagus-Acer*) or "maple-hemlock" (*Acer-Tsuga*) that were common in the FIA data, but we did not have the species well-replicated in our co-occurring tree-ring network and thus, we did not examine these species combinations.

Lastly, to evaluate the cumulative effect of droughts and pluvials for each forest type, we multiplied the magnitude of the drought and pluvial effects using 75th, 50th, and 25th percentiles (shown in Figure 2) of the range of effects sizes across the sites for each species with the number of occurrences over the observed period (1901–2015). We then scaled those cumulative effects across the different forest types. For future conditions, we conducted the same calculation using future climate projections for each climate scenario, where we used the same effect sizes but then multiplied by the number of occurrences of extreme events for each threshold for the future period (2016–2100). To make the comparison over the same number of years across the observed and the future projections, we shorten the observed record to 1931–2015.

2.6 | Mortality

To examine the role of mortality in the mesic eastern forests, we analyzed FIA data for the states of Indiana, Ohio, Pennsylvania, and New York, which cover a large portion of the tree-ring network used in this study. We gathered inventories from these states from 2001 to 2021 from plots that were inventoried every 5 years exactly, which resulted in 15,164 inventories across 5189 plots. We focused on the same species from the tree-ring network (i.e., *L. tulipifera*, *A. saccharum*, *C. ovata*, *Q. alba*, and *Q. rubra*) and examined trees with

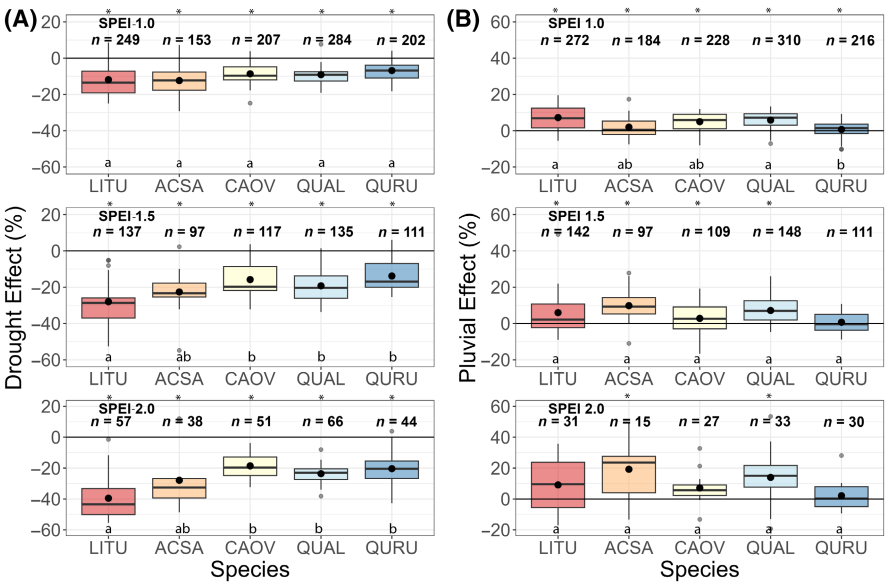

FIGURE 2 Species-level responses to hydroclimate extremes in eastern US forests. Effects of species growth to drought (A) and pluvial (B) conditions for seasonal (March–August average; August SPEI6) hydroclimate conditions for mild (SPEI6 = ±1.0; top), moderate (SPEI6 = ±1.5; middle), and extreme (SPEI6 = ±2.0; bottom) events. Lowercase lettering represents statistical significance differences in effect size between species via an ANOVA analysis Tukey HSD post hoc test. Asterisks represent the mean is significantly ($p \leq .05$) different from zero using a one-sample *t*-test. The sample size of the number of extremes experienced by each species is denoted. ACSA, *Acer saccharum*; CAOV, *Carya ovata*; LITU, *Liriodendron tulipifera*; QUAL, *Quercus alba*; QURU, *Quercus rubra*.

a diameter greater than 12.7 cm, to ensure we removed most of the subcanopy trees in order to better match with our tree ring network.

In each plot, we calculated the basal area (BA) change associated with growth between successive inventories among the exact same individuals. We calculated basal area change associated with mortality by summing basal area lost when trees died between successive inventories. We multiplied the basal area change by −1 to indicate this basal area was lost since the last inventory. We then matched the FIA plots to the SPEI 0.5°×0.5° gridded data boundaries and calculated the mean August SPEI6 change between inventories. Lastly, we evaluated the basal area change across different SPEI6 conditions. Because we had to average SPEI over a 5-year period due to the inventory recurrence, it muted extremes in the SPEI metric. Regardless, we can still examine losses in BA from mortality and compare them to increases in BA due to growth.

2.7 | Future projections

To examine how future climate change could impact species-specific responses to extreme wet and dry conditions, we extracted climate projections from 12 global climate models (GCMs) from the Coupled Model Intercomparison Project—Phase 6 (CMIP6; Eyring et al., 2016) listed in Table S2 and for four Shared socio-economic pathways (SSP) that include low (SSP1–2.6), moderate-low (2–4.5), moderate-high (3–7.0), and high (5–8.5) emission pathways (O'Neill et al., 2016). The CMIP6 models generally capture observed global and regional patterns of temperature and precipitation extremes (Kim et al., 2020), with greater accuracy when the ensemble mean is assessed (Srivastava et al., 2020). Additionally, CMIP6 models predict similar trends in droughts as the older CMIP5 models (Cook et al., 2020), suggesting a robust finding that droughts are likely to increase in magnitude and frequency. For each GCM, we extracted average monthly air temperature, precipitation, and the variables needed to estimate reference evapotranspiration (Allen et al., 2006), which include maximum air temperature, minimum air temperature, wind speed, relative humidity (used to estimate vapor pressure deficit), and incoming solar radiation (used to estimate net solar radiation). After bi-linearly interpolating each GCM to a common 1.5° grid, climate data for the nearest GCM grid node to each forest stand were extracted.

We used the ensemble mean of the monthly mean precipitation along with reference evapotranspiration (Allen et al., 2006) averaged across the growing season months (March–August), to calculate SPEI using the "SPEI" package in R (Beguería et al., 2014; Vicente-Serrano et al., 2010). The parameters of the log-logistic distribution used to estimate SPEI were calculated using the instrumental period (1901–2015). Because the ensemble mean of the future climate conditions has muted interannual variance compared to the instrumentally recorded data, we bias-corrected the projected SPEI after fitting the SPEI distribution using the climate model outputs. The time series of SPEI had both positive and negative biases across its cumulative probability distribution (Figure S1); thus, we used quantile mapping to bias correct the projected SPEI for each site (Ficklin et al., 2016; Robeson et al., 2020) with the "RQUANT" method in the "QMAP" package in R (Gudmundsson et al., 2012).

3 | RESULTS

3.1 | Drought and pluvial effects

Of the five species examined, the growth of *L. tulipifera* was most sensitive to drought, with a median drought effect ranging from a 19% decrease in growth during mild droughts to a 53% decrease during extreme droughts. During mild droughts (using the seasonal August SPEI6 = −1.0), all species had a similar growth decrease (Figure 2a). As the drought intensity threshold increased, drought response differences across species expanded in effect size and *L. tulipifera* was significantly ($p < .05$) different from *C. ovata*, *Q. alba*, and *Q. rubra* (Figure 2a). The average drought effect of *L. tulipifera* and *A. saccharum* was two times greater than for the *Quercus* and *Carya* species during extreme droughts, while the difference is only 1.25 times greater during mild droughts. The same pattern existed when examining shorter drought durations (i.e., SPEI1 and SPEI3), where all species experienced similar growth decreases during mild droughts but as drought increased, *L. tulipifera* consistently experienced significantly greater decreases in growth during drought while *A. saccharum* had an intermediate response, and *C. ovata* and the *Quercus* species had smaller growth decreases (Figures S2 and S3).

The pluvial effects were relatively smaller in magnitude (all less than 20% increases in growth) than drought responses, and there were few differences in pluvial response among species (Figure 2b). As pluvial intensity increased, growth generally remained the same or marginally increased (Figure 2b). Furthermore, the lack of species-specific response remained as pluvial intensity increased, although the variance of the response increased to the point that only *A. saccharum* and *Q. alba* had responses significantly different than zero (Figure 2b). This same pattern occurred during shorter pluvial durations (SPEI1 and SPEI3), with increased variance in the pluvial response with increased intensity and a lack of a species-specific response (Figures S4 and S5). In all cases, the pluvial response was smaller than the drought response.

3.2 | Sensitivity to climatic extremes

When examining the slope of the nonlinear relationship between growth and the full spectrum of growing season SPEI (not just the extremes), we find similar species-specific responses (Figure 3; Table S1). *L. tulipifera* has the steepest slope followed by *A. saccharum*, *Q. alba*, *C. ovata*, and *Q. rubra* during drought conditions (Figure 3). Slopes during pluvial conditions were marginally positive or flat during mild wet conditions and shifted to more negative slopes when pluvial conditions increased in intensity for all species (Figure 3).

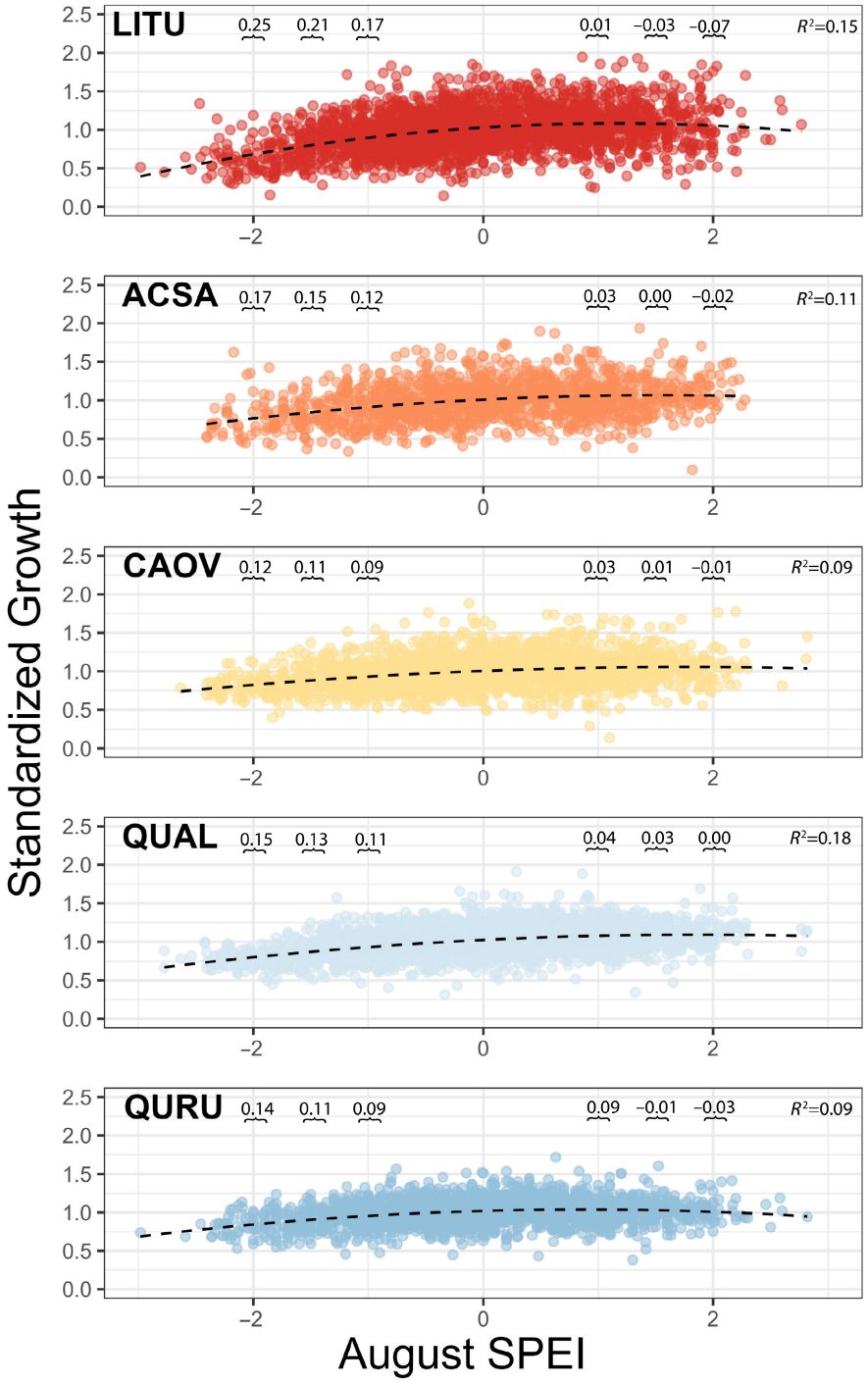

FIGURE 3 The relationship between standardized growth and March–August SPEI (August SPEI6) values for each species. Dashed line is the ordinary least-squares quadratic regression whose slope (ΔSRW/ΔSPEI) at SPEI values of −2.0, −1.5, −1.0, 1.0, 1.5, and 2.0 along with multiple R^2 are given in each panel. ACSA, *Acer saccharum*; CAOV, *Carya ovata*; LITU, *Liriodendron tulipifera*; QUAL, *Quercus alba*; QURU, *Quercus rubra*.

The growth differential percentage indicates that *L. tulipifera* growth post drought is the closest to (but still below) the pre-drought level (Figure 4) across the two lower drought intensity thresholds; however, *A. saccharum* has higher growth after the most extreme droughts. Interestingly, we see species-specific patterns in growth after drought throughout the various drought intensities (Figure 4). However, for more intense droughts, species-specific responses become more pronounced with the general pattern that growth from *L. tulipifera* and *A. saccharum* is closer to predrought conditions, while *C. ovata*, *Q. alba*, and *Q. rubra* have less growth compared to predrought conditions (Figure 4). When examining how growth returns to normal from wet events (Figure S6), the growth differential percentage has generally lower negative percentages (i.e., above the pre-pluvial growth conditions) with few differences among species. As conditions get wetter, we see a weaker growth differential percentage with only *Q. alba* having a growth differential percentage different from zero during the most extreme pluvials.

3.3 | Forest response

When scaled to represent various species compositions of canopy-dominant trees throughout the eastern United States, we found

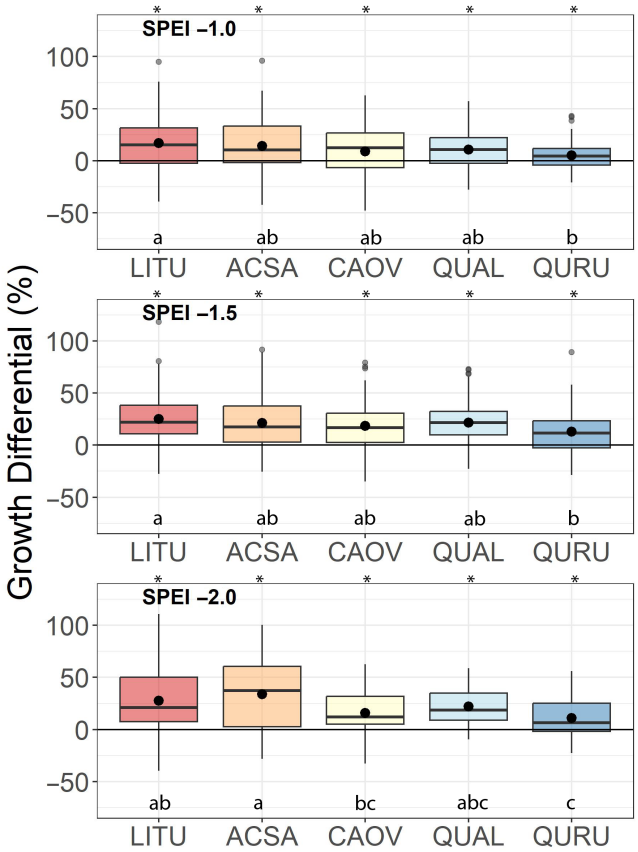

FIGURE 4 Growth differential percentage from drought index for each species. The growth differential percentage is averaged from the 2 years after drought and accounts for the weighting of drought impacts on growth. A higher mean growth differential percentage indicates growth closer to the pre-drought conditions. Lettering represents statistical significance differences in effect size between species via an ANOVA analysis Tukey HSD post hoc test. Asterisks represent the mean is significantly higher than zero using a one-sample *t*-test. ACSA, *Acer saccharum*; CAOV, *Carya ovata*; LITU, *Liriodendron tulipifera*; QUAL, *Quercus alba*; QURU, *Quercus rubra*.

that the scaled weighted means did not differ significantly among forest types, in part due to all species being present in all forest types but just in different proportions. However, the xeric species makeup (80% *Quercus–Carya*) had the smallest mean growth reduction (14.5%) to drought compared to the other forest compositions (15.9%–18.7%) across drought intensities for the growing season (August SPEI6) (Figure 5). The mesic species makeup (80% *Acer–Liriodendron*) had the highest mean growth reduction at 18.7%. Thus, more intense droughts have a larger (up to 8% total) impact on growth for mesic dominant forests compared to xeric (Figure 5). In all forest types, mild droughts had significantly lower negative effects on growth than moderate or extreme droughts. For pluvials, we see that xeric forests have the smallest increase in growth and mesic forests have the largest increases. In all cases, the increases in growth from pluvials are smaller than the decreases during drought (Figure 5). In terms of growth differential percentage, forests composed of mesic species have higher growth differential percentages than xeric forests, particularly for extreme droughts (Figure 5). The return to normal growth from pluvial conditions is modest with large errors, independent of the intensity of the pluvial event (Figure 5).

3.4 | Mortality versus growth effects on stand basal area change

For each species across all SPEI conditions, increases in stand basal area from growth between successive inventories far outweighed the decreases in basal area from mortality (Figure 6). Due to the 5-year interval in FIA plot inventories, the range of SPEI conditions is fairly limited, but in general, we find that growth is slightly higher (but not significantly different) during the drier and normal conditions, while growth is lowest during the wettest conditions (due to 5-year interval muting SPEI variance, all conditions would be classified as normal in the tree ring analysis), supporting the nonlinear response from the tree ring data. For mortality, we see more basal area decrease during drier conditions compared to wetter conditions (Figure 6).

3.5 | Future climate

The ensemble of the climate models projects a drier climate in the future (2016–2100) for all scenarios across the 37 sites, ranging from a mean decrease in SPEI of −0.38 (SSPI −2.6) to −1.00 (SSP5–8.5) in August SPEI6 (Figure S7). In addition to a shift in mean conditions, the distribution of SPEI values changes depending on concentration scenario and drought or pluvial category (Figure S7). On the wet tail of the distribution, we see very little change across scenarios and only marginal changes from the observed period, although the mildly wet SPEI values become much less frequent (2–5 times less frequent depending on the scenario) compared to the observed period (Table S3). On the drier side of the distribution, we see dramatic shifts in occurrence for mild, moderate, and extreme droughts (SPEI = −1.0, −1.5, and −2.0, respectively). Regardless of the scenario, all droughts are projected to be much more frequent. The likelihood ratio for the mild droughts results in a 3–20 times increase in occurrence (Table S3), depending on the scenario of warming, while the moderate and extreme droughts see dramatic increases but to a lesser extent (3–9 times and 3–5 times more likely, respectively) (Table S3). Thus, the largest, most likely changes are decreases in mild wet events and increases in all dry events, especially mild droughts.

While the effect size is an important feature, the frequency of an extreme event occurrence is also critical when thinking about the overall impact of extremes over time. Due to their higher frequency during the observed period, mild droughts have a much larger cumulative effect on growth than do more extreme droughts (Figure 7a). Similarly, mild pluvials lead to a larger cumulative effect on growth due the increased frequency of occurrence, albeit a smaller overall

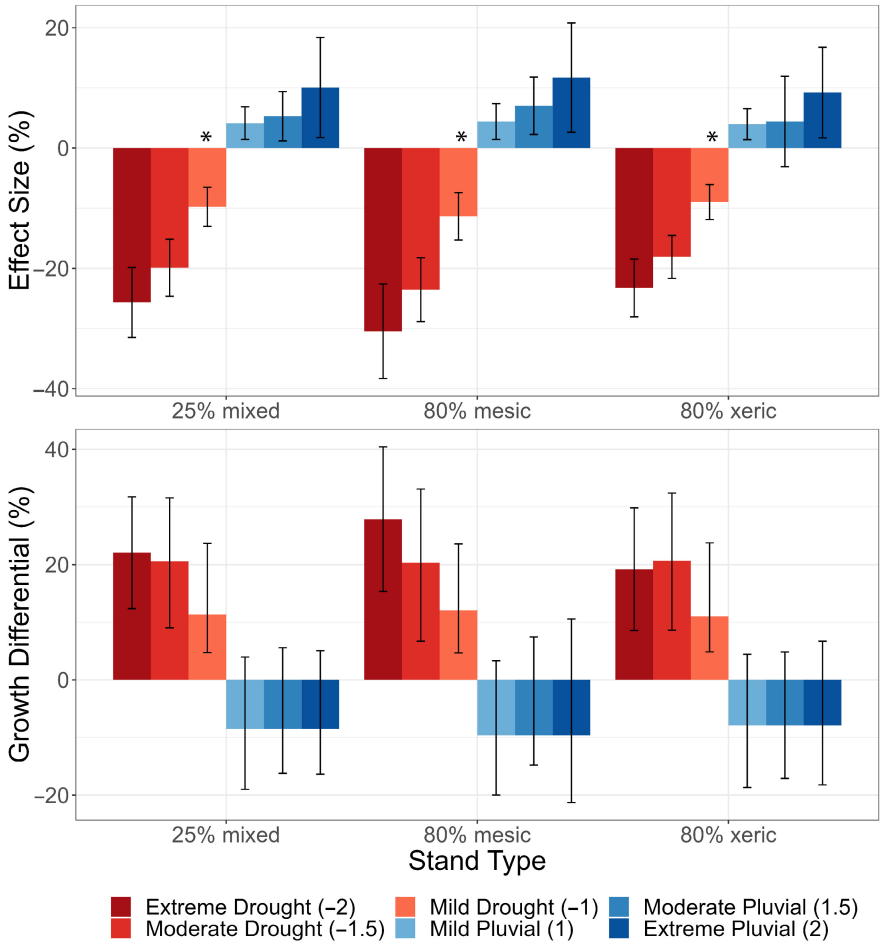

FIGURE 5 Effect size and growth differential percentage for Eastern Deciduous Forest species under hydroclimate extremes. (Top) Pluvial and drought effect sizes for scaled canopy dominant species composition scenarios across intensity thresholds, with error bars. (Bottom) Growth differential percentage percentages for scaled canopy-dominant species composition scenarios across intensity thresholds, with error bars. Xeric = 80% of canopy dominant trees are *Quercus* and *Carya*; Mesic = 80% of trees are *Acer* and *Liriodendron*; Mixed = *Quercus*, *Carya*, *Liriodendron*, and *Acer* each make up 25% of the forest. Asterisk indicates significantly different from other drought categories.

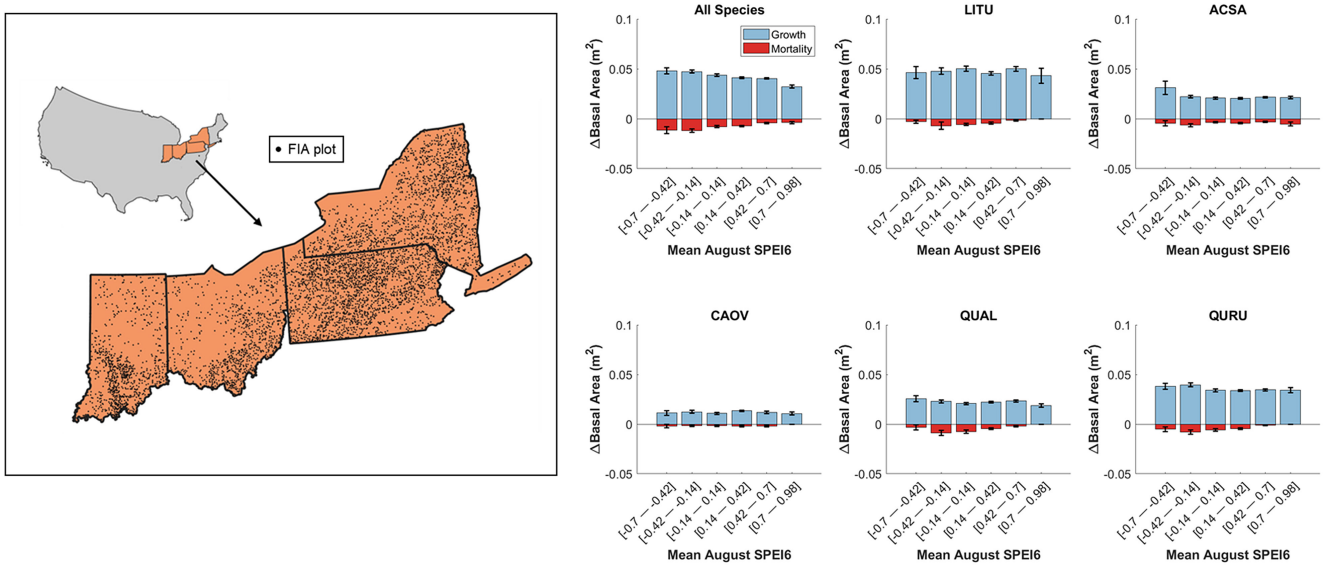

FIGURE 6 USDA Forest Inventory Analysis plots (left) were used to determine the basal area change between inventories to compare the positive effect of growth (blue) on basal area to the negative effect of mortality (red) across different SPEI conditions for all species and each studied species. ACSA, *Acer saccharum*; CAOV, *Carya ovata*; LITU, *Liriodendron tulipifera*; QUAL, *Quercus alba*; QURU, *Quercus rubra*.

effect compared to drought decreases. Of the various forest types, mesic forests are the most affected by changes in extremes with drought having a larger impact than pluvials (Figure 7a,b).

Increased frequencies of hydroclimatic extremes in the future increase the cumulative effect that drought has on growth, especially for the mesic forest type (Figure 7c,d). All climate scenarios indicate

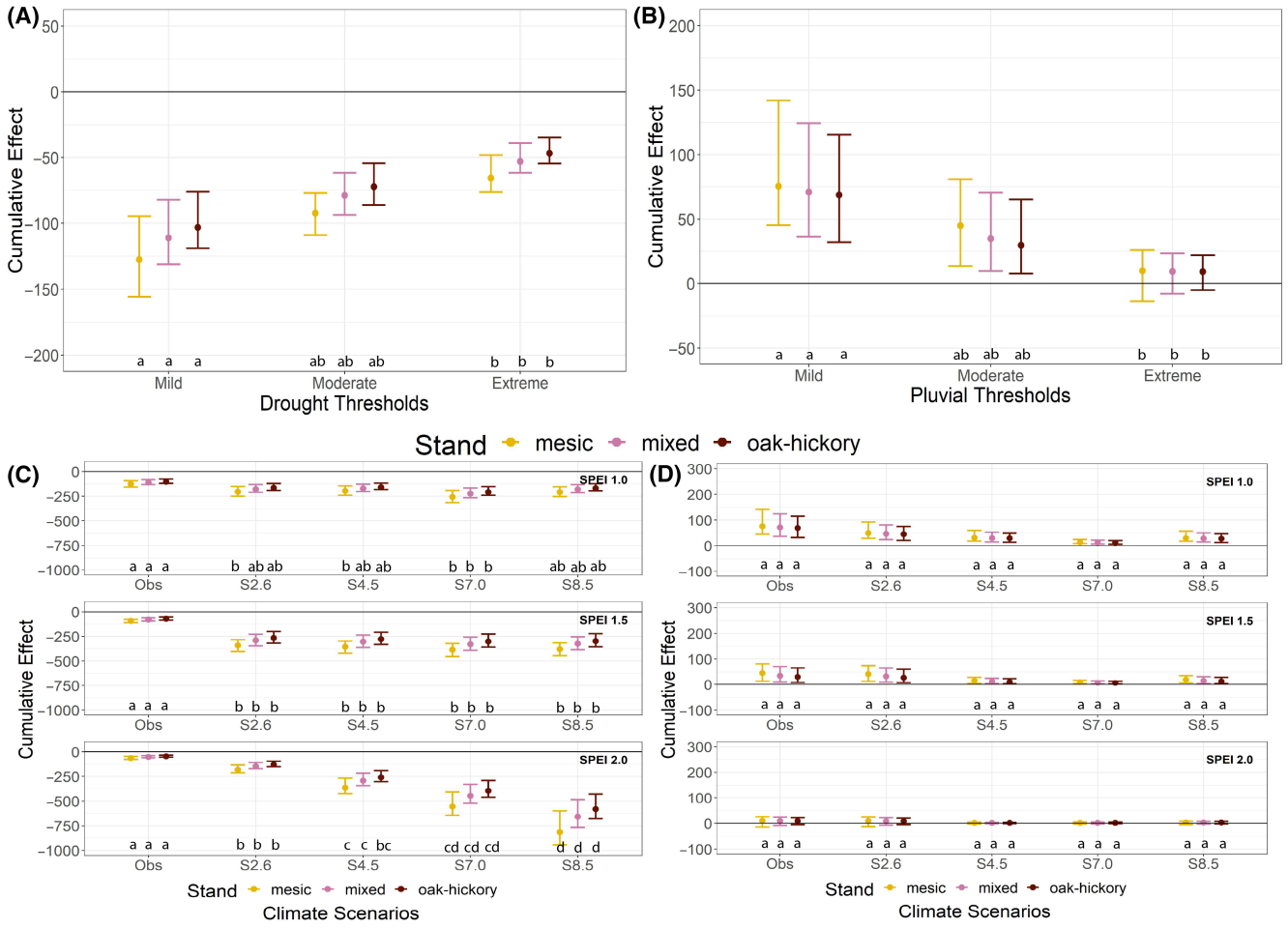

FIGURE 7 Cumulative effects (effect size multiplied by the number of events) of hydroclimate extremes on species growth for the observed (1901–2016) across each drought (A) and pluvial (B) thresholds and for each future (2016–2100) climate scenario of the 75th, 50th, and 25th quantities for droughts (C) and pluvials (D). Lettering represents statistical significance differences in effect size between species via an ANOVA analysis Tukey HSD post hoc test.

an increase in frequency of all drought categories (Figure S7); thus, we see significant increases in the cumulative effect of drought across all scenarios with increasing cumulative effects as warming increases. Conversely, more warming leads to less frequent pluvials (likely driven by water demand); thus, we see larger effects in the lower warming scenarios (SSP1–2.6 and SSP2–4.5), but in all cases, the effect is smaller than in the observed period and not significantly different. Furthermore, the overall effect size is substantially smaller than the drought cumulative effect (Figure 7).

4 | DISCUSSION

We found that the negative effects of drought on growth are larger than the positive effects of pluvials (Figures 2 and 7), supporting assertions that nonlinear climate-growth responses are predominant in forests (Dannenberg et al., 2019) including in the eastern United States (Anderson-Teixeira et al., 2022; Rollinson et al., 2021). If we assumed a linear relationship, the drought response would have been underestimated (by 2–3 times), and the pluvial response would have been overestimated compared to the nonlinearly estimated responses (Table S1). These findings are likely due to soil saturation during pluvials and/or water is no longer a limiting factor of growth thus, adding more water does not lead to more growth. In extreme cases, when soils become waterlogged, oxygen is depleted, which can decrease growth (Kreuzwieser et al., 2004). Both scenarios highlight the importance of accurately modeling the asymmetric climate-growth responses of trees, with implications for estimating impacts to carbon sequestration. Such asymmetric responses across the five studied species indicate that carbon lost from drought-induced radial growth declines is not compensated by increases in growth during wet periods in the eastern United States (Figures 2 and 7).

The magnitude of the growth response to drought reveals species-specific responses for all drought intensities. The effect size and the difference of the mean effect size between species increased with drought intensity (Figure 2). Previous research on species-specific growth responses to drought demonstrates mixed results. Some studies found little to no difference in growth responses to drought among species in eastern US forests (e.g., LeBlanc & Terrell, 2011; Martin-Benito & Pederson, 2015). These studies often used

correlation analyses and compared responses between species situated across various locations of their respective range, confounding analyses of their drought sensitivity. Other studies that focused on the magnitude of the growth response and examined species that were located in the same landscape positions found that species-specific growth responses to drought depended on water-use strategy, with those being more conservative (isohydric) having greater growth sensitivity to drought (Au et al., 2020; Brzostek et al., 2014; Elliott et al., 2015; Lockwood et al., 2023; Novick et al., 2022). While others have hypothesized that species-specific differences in growth response to drought intensity would increase in a warming climate (e.g., Elliott et al., 2015), little to no evidence has been presented to support that hypothesis. Here, we find support for this hypothesis, finding that species-specific responses increase with drought intensity, likely due to changes in the water table (Brzostek et al., 2014). During mild droughts, all trees have some access to water and thus have smaller growth decreases. During extreme droughts, all species are impacted but those with shallow roots, such as *L. tulipifera* and *A. saccharum* (Brzostek et al., 2014), have an even larger decrease in growth (Figure 2).

While species-specific responses are prevalent in the moderate and extreme drought intensities, the cumulative impact of mild droughts on growth is larger due to their greater frequency (Figure 7). Eastern US forests are composed of several species that employ various water-use strategies, thus drought conditions can impact certain forest types more than others. Forest stands that have a larger component of mesic species, such as *A. saccharum* and *L. tulipifera*, have larger growth reductions during moderate and extreme droughts compared to those stands with larger proportions of xeric species, such as those in the *Quercus* and *Carya* genera (Figure 7). However, we found the growth differential percentage from the mesic species is higher and thus growth after drought is closer to the pre-drought growth compared to xeric species (Figure 4). This is in part because all species returned close to pre-drought growth after 1 year, resulting in larger growth differential from the mesic species because they had larger drought effects. Nevertheless, drought will have a larger impact on growth in forests with mesic species but with shorter drought legacies in the years following drought. These nonlinear and species-specific growth responses are important to include in vegetation models to increase our ability to predict how climate will impact forests in the future.

Climate models project a drier climate with more frequent drought in the future in eastern US forests across all scenarios (Figure S7), even those with aggressive mitigation (e.g., SSP1–2.6). Given that even moderate droughts have a large impact on species-specific growth responses, the future is very likely to see an increase in differential responses of forest growth to drought, making understanding species responses to climate even more important in the future. In the higher emissions scenarios (SSP3–7.0 and SSP5–8.5), increases in the frequency of extreme drought could have a cumulative effect approximately five times greater than that of the observed period. Depending on the emission scenario of the future, the relative growth after extremes could also see more species-specific responses (Figure 5). The higher emission scenarios show mesic species returning to pre-drought growth better than the xeric species. Thus, future warming will impact both the growth response during and after extremes, but the intensity of future droughts will determine the degree of species-specific impacts from drought and thus the impact to forest stands with various species composition. We note that this study does not account for any acclimation/adaptation of a given species or new species compositions, something important to consider as we try to better understand how forests will respond to ongoing climate change.

Stem growth is the main above-ground carbon pool (Fahey et al., 2010), and thus, tree-ring responses to climate have large carbon implications (Babst et al., 2014). Compared to variations in photosynthetic processes, drought has a much larger impact on growth (Cabon et al., 2022; Dow et al., 2022) and mortality (Martinez-Vilalta et al., 2019), so drought particularly affects long residence carbon stored from growth and has the potential to reduce the residence time of carbon and impact the amount of carbon that forests sequester (Kannenberg et al., 2022). Our results indicate that as the demographic shift from xeric to mesic species continues throughout large portions of the eastern United States (Abrams, 2003; McEwan et al., 2011; Novick et al., 2022), drought will have a larger impact on growth and thus carbon storage. While drought-induced mortality is relatively less common in the mesic eastern United States, mortality remains an important component of the carbon budget. Here, we find that basal area changes from growth far outweigh those to mortality (Figure 6), indicating that drought-induced growth reductions in the mesic eastern United States likely have a larger impact on the carbon budget than drought-induced mortality, at least under present climatic conditions. This is in part due to the complex number of variables that lead to mortality. Generally, drought is rarely extreme enough to induce mortality outright but is more often a contributor to mortality alongside other variables such as pest infestations (McDowell et al., 2011). However, the need to better understand the role of mortality in the overall above-ground carbon budget remains critical to get a more complete picture of how climate impacts carbon pools in mesic forests. Furthermore, as droughts become more intense in the future, growth response to climate could change. Moreover, if droughts are extreme enough, drought-induced mortality could become widespread, causing large changes in ecosystem structure and composition beyond just growth declines. Thus, a better understanding of what climatic threshold causes mortality will lead to a more accurate projection of how future climate change will impact these mesic forests.

5 | CONCLUSIONS

Across deciduous forests of the eastern United States, we found that mesic species such as *L. tulipifera* and *A. saccharum* were more sensitive to drought across all drought intensities. Furthermore, growth responded asymmetrically to drought, with the positive growth response to pluvials failing to outweigh reductions of

growth during drought. When accounting for forest species composition, forests dominated by mesic species show greater reductions in growth during drought but also higher growth differential percentages. Thus, the ongoing increase in mesic species in eastern US forests in combination with the likely increase in drought conditions, suggest that drought will likely have a larger impact on the carbon uptake in the future in the eastern United States. However, these same forests showed higher growth differential percentages following droughts compared to those that are dominated by xeric species. Regardless, the combination of more mesic species and a warmer future with more frequent droughts will result in more drought-induced carbon losses from a forest that is a tremendous carbon sink.

AUTHOR CONTRIBUTIONS

Justin T. Maxwell: Conceptualization; data curation; formal analysis; funding acquisition; investigation; methodology; project administration; supervision; visualization; writing – original draft; writing – review and editing. **Tsun Fung Au:** Conceptualization; formal analysis; methodology; writing – review and editing. **Steven A. Kannenberg:** Conceptualization; investigation; methodology; writing – review and editing. **Grant L. Harley:** Funding acquisition; visualization; writing – review and editing. **Matthew P. Dannenberg:** Formal analysis; methodology; writing – review and editing. **Darren L. Ficklin:** Formal analysis; methodology; writing – review and editing. **Scott M. Robeson:** Formal analysis; methodology; writing – review and editing. **Macarena Férriz:** Data curation; writing – review and editing. **Michael C. Benson:** Formal analysis; visualization; writing – review and editing. **Benjamin R. Lockwood:** Data curation; methodology; writing – review and editing. **Kimberly A. Novick:** Funding acquisition; writing – review and editing. **Richard P. Phillips:** Funding acquisition; writing – review and editing. **Maegen L. Rochner:** Writing – review and editing. **Neil Pederson:** Conceptualization; investigation; project administration; writing – review and editing.

ACKNOWLEDGEMENTS

We thank Josh Bregy, James Dickens, James McGee, Josh Oliver, Karly Schmidt-Simard, Brynn Taylor, Brandon Strange, Michael Thornton, Senna Robeson, Matt Wenzel, and Luke Wylie for assistance in the field and lab. We also would like to acknowledge the following funding: USDA Agriculture and Food Research Initiative grant 2017-67013-26191, National Science Foundation, P2C2 Program AGS-1805617 and AGS-1805276, the Harvard Forest Bullard Fellowship, Harvard University, and Indiana University Vice Provost for Research Faculty Research Program. We acknowledge the World Climate Research Programme, which, through its Working Group on Coupled Modelling, coordinated and promoted CMIP6. We thank the climate modeling groups for producing and making available their model output, the Earth System Grid Federation (ESGF) for archiving the data and providing access, and the multiple funding agencies who support CMIP6 and ESGF.

CONFLICT OF INTEREST STATEMENT

The authors declare that there is no conflict of interest.

DATA AVAILABILITY STATEMENT

The tree-ring chronologies are publicly available at the International Tree-Ring Data Bank (https://www.ncei.noaa.gov/products/paleoclimatology/tree-ring). The Standardized Precipitation Evapotranspiration data is publicly available at https://spei.csic.es/index.html. A list of the Global Climate Models used to get the ensemble mean for future conditions is listed in Table S2.

ORCID

Justin T. Maxwell https://orcid.org/0000-0001-9195-3146
Tsun Fung Au https://orcid.org/0000-0003-0591-9342
Matthew P. Dannenberg https://orcid.org/0000-0002-6518-4897
Kimberly A. Novick https://orcid.org/0000-0002-8431-0879

REFERENCES

Abrams, M. D. (2003). Where has all the white oak gone? *Bioscience*, *53*(10), 927–939. https://doi.org/10.1641/0006-3568(2003)053[0927:WHATWO]2.0.CO;2

Alexander, M. R., Rollinson, C. R., Babst, F., Trouet, V., & Moore, D. J. P. (2018). Relative influences of multiple sources of uncertainty on cumulative and incremental tree-ring-derived aboveground biomass estimates. *Trees*, *32*(1), 265–276. https://doi.org/10.1007/s00468-017-1629-0

Allen, C. D., Macalady, A. K., Chenchouni, H., Bachelet, D., McDowell, N., Vennetier, M., Kitzberger, T., Rigling, A., Breshears, D. D., Hogg, E. H., Gonzalez, P., Fensham, R., Zhang, Z., Castro, J., Demidova, N., Lim, J.-H., Allard, G., Running, S. W., Semerci, A., & Cobb, N. (2010). A global overview of drought and heat-induced tree mortality reveals emerging climate change risks for forests. *Forest Ecology and Management*, *259*(4), 660–684. https://doi.org/10.1016/j.foreco.2009.09.001

Allen, R. G., Pruitt, W. O., Wright, J. L., Howell, T. A., Ventura, F., Snyder, R., Itenfisu, D., Steduto, P., Berengena, J., Yrisarry, J. B., Smith, M., Pereira, L. S., Raes, D., Perrier, A., Alves, I., Walter, I., & Elliott, R. (2006). A recommendation on standardized surface resistance for hourly calculation of reference ETo by the FAO56 Penman-Monteith method. *Agricultural Water Management*, *81*(1), 1–22. https://doi.org/10.1016/j.agwat.2005.03.007

Anderegg, W. R. L., Konings, A. G., Trugman, A. T., Yu, K., Bowling, D. R., Gabbitas, R., Karp, D. S., Pacala, S., Sperry, J. S., Sulman, B. N., & Zenes, N. (2018). Hydraulic diversity of forests regulates ecosystem resilience during drought. *Nature*, *561*(7724), 538–541. https://doi.org/10.1038/s41586-018-0539-7

Anderson-Teixeira, K. J., Herrmann, V., Rollinson, C. R., Gonzalez, B., Gonzalez-Akre, E. B., Pederson, N., Alexander, M. R., Allen, C. D., Alfaro-Sánchez, R., Awada, T., Baltzer, J. L., Baker, P. J., Birch, J. D., Bunyavejchewin, S., Cherubini, P., Davies, S. J., Dow, C., Helcoski, R., Kašpar, J., … Zuidema, P. A. (2022). Joint effects of climate, tree size, and year on annual tree growth derived from tree-ring records of ten globally distributed forests. *Global Change Biology*, *28*(1), 245–266. https://doi.org/10.1111/gcb.15934

Au, T. F., & Maxwell, J. T. (2022). Drought sensitivity and resilience of oak–hickory stands in the eastern United States. *Forests*, *13*(3), 3. https://doi.org/10.3390/f13030389

Au, T. F., Maxwell, J. T., Novick, K. A., Robeson, S. M., Warner, S. M., Lockwood, B. R., Phillips, R. P., Harley, G. L., Telewski, F. W.,

Therrell, M. D., & Pederson, N. (2020). Demographic shifts in eastern US forests increase the impact of late-season drought on forest growth. *Ecography*, *43*(10), 1475–1486. https://doi.org/10.1111/ecog.05055

Au, T. F., Maxwell, J. T., Robeson, S. M., Li, J., Siani, S. M. O., Novick, K. A., Dannenberg, M. P., Phillips, R. P., Li, T., Chen, Z., & Lenoir, J. (2022). Younger trees in the upper canopy are more sensitive but also more resilient to drought. *Nature Climate Change*, *12*(12), 1168–1174. https://doi.org/10.1038/s41558-022-01528-w

Babst, F., Alexander, M. R., Szejner, P., Bouriaud, O., Klesse, S., Roden, J., Ciais, P., Poulter, B., Frank, D., Moore, D. J. P., & Trouet, V. (2014). A tree-ring perspective on the terrestrial carbon cycle. *Oecologia*, *176*(2), 307–322. https://doi.org/10.1007/s00442-014-3031-6

Barnes, M. L., Zhang, Q., Robeson, S. M., Young, L., Burakowski, E. A., Oishi, A. C., Stoy, P. C., Katul, G., & Novick, K. A. (2024). A century of reforestation reduced anthropogenic warming in the eastern United States. *Earth's Future*, *12*(2), e2023EF003663. https://doi.org/10.1029/2023EF003663

Beguería, S., Vicente-Serrano, S. M., Reig, F., & Latorre, B. (2014). Standardized precipitation evapotranspiration index (SPEI) revisited: Parameter fitting, evapotranspiration models, tools, datasets and drought monitoring. *International Journal of Climatology*, *34*(10), 3001–3023. https://doi.org/10.1002/joc.3887

Bennett, L. T., Bruce, M. J., Machunter, J., Kohout, M., Krishnaraj, S. J., & Aponte, C. (2017). Assessing fire impacts on the carbon stability of fire-tolerant forests. *Ecological Applications*, *27*(8), 2497–2513.

Breshears, D. D., Cobb, N. S., Rich, P. M., Price, K. P., Allen, C. D., Balice, R. G., Romme, W. H., Kastens, J. H., Floyd, M. L., Belnap, J., Anderson, J. J., Myers, O. B., & Meyer, C. W. (2005). Regional vegetation die-off in response to global-change-type drought. *Proceedings of the National Academy of Sciences*, *102*(42), 15144–15148. https://doi.org/10.1073/pnas.0505734102

Brzostek, E. R., Dragoni, D., Schmid, H. P., Rahman, A. F., Sims, D., Wayson, C. A., Johnson, D. J., & Phillips, R. P. (2014). Chronic water stress reduces tree growth and the carbon sink of deciduous hardwood forests. *Global Change Biology*, *20*(8), 2531–2539. https://doi.org/10.1111/gcb.12528

Bussberg, N. W., Maxwell, J. T., Robeson, S. M., & Huang, C. (2020). The effect of end-point adjustments on smoothing splines used for tree-ring standardization. *Dendrochronologia*, *60*, 125665. https://doi.org/10.1016/j.dendro.2020.125665

Cabon, A., Kannenberg, S. A., Arain, A., Babst, F., Baldocchi, D., Belmecheri, S., Delpierre, N., Guerrieri, R., Maxwell, J. T., McKenzie, S., Meinzer, F. C., Moore, D. J. P., Pappas, C., Rocha, A. V., Szejner, P., Ueyama, M., Ulrich, D., Vincke, C., Voelker, S. L., … Anderegg, W. R. L. (2022). Cross-biome synthesis of source versus sink limits to tree growth. *Science*, *376*(6594), 758–761. https://doi.org/10.1126/science.abm4875

Cook, B. I., Mankin, J. S., Marvel, K., Williams, A. P., Smerdon, J. E., & Anchukaitis, K. J. (2020). Twenty-first century drought projections in the CMIP6 forcing scenarios. *Earth's Future*, *8*(6), e2019EF001461.

Cook, E. R. (1985). *A time series analysis approach to tree ring standardization*. The University of Arizona.

Cook, E. R., & Peters, K. (1981). *The smoothing spline: A new approach to standardizing forest interior tree-ring width series for dendroclimatic studies*. https://repository.arizona.edu/handle/10150/261038

Costanza, J. K., Koch, F. H., & Reeves, M. C. (2023). Future exposure of forest ecosystems to multi-year drought in the United States. *Ecosphere*, *14*(5), e4525. https://doi.org/10.1002/ecs2.4525

Dannenberg, M. P., Wise, E. K., & Smith, W. K. (2019). Reduced tree growth in the semiarid United States due to asymmetric responses to intensifying precipitation extremes. *Science Advances*, *5*(10), eaaw0667. https://doi.org/10.1126/sciadv.aaw0667

Delpierre, N., Vitasse, Y., Chuine, I., Guillemot, J., Bazot, S., Rutishauser, T., & Rathgeber, C. B. K. (2016). Temperate and boreal forest tree phenology: From organ-scale processes to terrestrial ecosystem models. *Annals of Forest Science*, *73*(1), 5–25. https://doi.org/10.1007/s13595-015-0477-6

D'Orangeville, L., Maxwell, J., Kneeshaw, D., Pederson, N., Duchesne, L., Logan, T., Houle, D., Arseneault, D., Beier, C. M., Bishop, D. A., Druckenbrod, D., Fraver, S., Girard, F., Halman, J., Hansen, C., Hart, J. L., Hartmann, H., Kaye, M., Leblanc, D., … Phillips, R. P. (2018). Drought timing and local climate determine the sensitivity of eastern temperate forests to drought. *Global Change Biology*, *24*(6), 2339–2351. https://doi.org/10.1111/gcb.14096

Dow, C., Kim, A. Y., D'Orangeville, L., Gonzalez-Akre, E. B., Helcoski, R., Herrmann, V., Harley, G. L., Maxwell, J. T., McGregor, I. R., McShea, W. J., McMahon, S. M., Pederson, N., Tepley, A. J., & Anderson-Teixeira, K. J. (2022). Warm springs alter timing but not total growth of temperate deciduous trees. *Nature*, *608*(7923), 552–557. https://doi.org/10.1038/s41586-022-05092-3

Dye, A., Barker Plotkin, A., Bishop, D., Pederson, N., Poulter, B., & Hessl, A. (2016). Comparing tree-ring and permanent plot estimates of aboveground net primary production in three eastern U.S. forests. *Ecosphere*, *7*(9), e01454. https://doi.org/10.1002/ecs2.1454

Eischeid, J. K., Hoerling, M. P., Quan, X. W., Kumar, A., Barsugli, J., Labe, Z. M., Kunkel, K. E., Schreck, C. J., III, Easterling, D. R., Zhang, T., & Uehling, J. (2023). Why has the summertime central US warming hole not disappeared? *Journal of Climate*, *36*(20), 7319–7336.

Elliott, K. J., Miniat, C. F., Pederson, N., & Laseter, S. H. (2015). Forest tree growth response to hydroclimate variability in the southern Appalachians. *Global Change Biology*, *21*(12), 4627–4641. https://doi.org/10.1111/gcb.13045

Eyring, V., Bony, S., Meehl, G. A., Senior, C. A., Stevens, B., Stouffer, R. J., & Taylor, K. E. (2016). Overview of the Coupled Model Intercomparison Project Phase 6 (CMIP6) experimental design and organization. *Geoscientific Model Development*, *9*(5), 1937–1958. https://doi.org/10.5194/gmd-9-1937-2016

Fahey, T. J., Woodbury, P. B., Battles, J. J., Goodale, C. L., Hamburg, S. P., Ollinger, S. V., & Woodall, C. W. (2010). Forest carbon storage: Ecology, management, and policy. *Frontiers in Ecology and the Environment*, *8*(5), 245–252. https://doi.org/10.1890/080169

Fei, S., Kong, N., Steiner, K. C., Moser, W. K., & Steiner, E. B. (2011). Change in oak abundance in the eastern United States from 1980 to 2008. *Forest Ecology and Management*, *262*(8), 1370–1377. https://doi.org/10.1016/j.foreco.2011.06.030

Ficklin, D. L., Abatzoglou, J. T., Robeson, S. M., & Dufficy, A. (2016). The influence of climate model biases on projections of aridity and drought. *Journal of Climate*, *29*(4), 1269–1285. https://doi.org/10.1175/JCLI-D-15-0439.1

Ficklin, D. L., & Novick, K. A. (2017). Historic and projected changes in vapor pressure deficit suggest a continental-scale drying of the United States atmosphere. *Journal of Geophysical Research: Atmospheres*, *122*(4), 2061–2079. https://doi.org/10.1002/2016JD025855

Ford, T. W. (2014). Precipitation anomalies in eastern-Central Iowa from 1640—Present. *Journal of Hydrology*, *519*, 918–924. https://doi.org/10.1016/j.jhydrol.2014.08.021

Grossiord, C., Buckley, T. N., Cernusak, L. A., Novick, K. A., Poulter, B., Siegwolf, R. T. W., Sperry, J. S., & McDowell, N. G. (2020). Plant responses to rising vapor pressure deficit. *New Phytologist*, *226*(6), 1550–1566. https://doi.org/10.1111/nph.16485

Gudmundsson, L., Bremnes, J. B., Haugen, J. E., & Engen-Skaugen, T. (2012). Technical note: Downscaling RCM precipitation to the station scale using statistical transformations—A comparison of methods. *Hydrology and Earth System Sciences*, *16*(9), 3383–3390. https://doi.org/10.5194/hess-16-3383-2012

Hamrick, J. L. (2004). Response of forest trees to global environmental changes. *Forest Ecology and Management*, *197*(1), 323–335. https://doi.org/10.1016/j.foreco.2004.05.023

Hoffmann, N., Schall, P., Ammer, C., Leder, B., & Vor, T. (2018). Drought sensitivity and stem growth variation of nine alien and native tree

species on a productive forest site in Germany. *Agricultural and Forest Meteorology*, *256–257*, 431–444. https://doi.org/10.1016/j.agrformet.2018.03.008

Holmes, R. L. (1983). Computer-assisted quality control in tree-ring dating and measurement. *Tree-Ring Bulletin*, *43*, 69–78.

Isbell, F., Craven, D., Connolly, J., Loreau, M., Schmid, B., Beierkuhnlein, C., Bezemer, T. M., Bonin, C., Bruelheide, H., de Luca, E., Ebeling, A., Griffin, J. N., Guo, Q., Hautier, Y., Hector, A., Jentsch, A., Kreyling, J., Lanta, V., Manning, P., … Eisenhauer, N. (2015). Biodiversity increases the resistance of ecosystem productivity to climate extremes. *Nature*, *526*(7574), 574–577. https://doi.org/10.1038/nature15374

Jiang, Y., Kim, J. B., Trugman, A. T., Kim, Y., & Still, C. J. (2019). Linking tree physiological constraints with predictions of carbon and water fluxes at an old-growth coniferous forest. *Ecosphere*, *10*(4), e02692. https://doi.org/10.1002/ecs2.2692

Kannenberg, S. A., Cabon, A., Babst, F., Belmecheri, S., Delpierre, N., Guerrieri, R., Maxwell, J. T., Meinzer, F. C., Moore, D. J. P., Pappas, C., Ueyama, M., Ulrich, D. E. M., Voelker, S. L., Woodruff, D. R., & Anderegg, W. R. L. (2022). Drought-induced decoupling between carbon uptake and tree growth impacts forest carbon turnover time. *Agricultural and Forest Meteorology*, *322*, 108996. https://doi.org/10.1016/j.agrformet.2022.108996

Kannenberg, S. A., Maxwell, J. T., Pederson, N., D'Orangeville, L., Ficklin, D. L., & Phillips, R. P. (2019). Drought legacies are dependent on water table depth, wood anatomy and drought timing across the eastern US. *Ecology Letters*, *22*(1), 119–127. https://doi.org/10.1111/ele.13173

Karl, T. R., Knight, R. W., Easterling, D. R., & Quayle, R. G. (1996). Indices of climate change for the United States. *Bulletin of the American Meteorological Society*, *77*(2), 279–292. https://doi.org/10.1175/1520-0477(1996)077<0279:IOCCFT>2.0.CO;2

Kim, Y. H., Min, S. K., Zhang, X., Sillmann, J., & Sandstad, M. (2020). Evaluation of the CMIP6 multi-model ensemble for climate extreme indices. *Weather and Climate Extremes*, *29*, 100269.

Kreuzwieser, J., Papadopoulou, E., & Rennenberg, H. (2004). Interaction of flooding with carbon metabolism of forest trees. *Plant Biology*, *6*(3), 299–306.

LeBlanc, D. C., & Terrell, M. A. (2011). Comparison of growth–climate relationships between northern red oak and white oak across eastern North America. *Canadian Journal of Forest Research*, *41*(10), 1936–1947. https://doi.org/10.1139/x11-118

Lloret, F., Keeling, E. G., & Sala, A. (2011). Components of tree resilience: Effects of successive low-growth episodes in old ponderosa pine forests. *Oikos*, *120*(12), 1909–1920. https://doi.org/10.1111/j.1600-0706.2011.19372.x

Lockwood, B. R., Maxwell, J. T., Denham, S. O., Robeson, S. M., LeBlanc, D. C., Pederson, N., Novick, K. A., & Au, T. F. (2023). Interspecific differences in drought and pluvial responses for *Quercus alba* and *Quercus rubra* across the eastern United States. *Agricultural and Forest Meteorology*, *340*, 109597. https://doi.org/10.1016/j.agrformet.2023.109597

Martin-Benito, D., & Pederson, N. (2015). Convergence in drought stress, but a divergence of climatic drivers across a latitudinal gradient in a temperate broadleaf forest. *Journal of Biogeography*, *42*(5), 925–937. https://doi.org/10.1111/jbi.12462

Martinez-Vilalta, J., Anderegg, W. R. L., Sapes, G., & Sala, A. (2019). Greater focus on water pools may improve our ability to understand and anticipate drought-induced mortality in plants. *New Phytologist*, *223*(1), 22–32. https://doi.org/10.1111/nph.15644

Mascioli, N. R., Previdi, M., Fiore, A. M., & Ting, M. (2017). Timing and seasonality of the United States 'warming hole'. *Environmental Research Letters*, *12*(3), 034008.

Maxwell, J. T., & Harley, G. L. (2017). Increased tree-ring network density reveals more precise estimations of sub-regional hydroclimate variability and climate dynamics in the Midwest, USA. *Climate Dynamics*, *49*(4), 1479–1493. https://doi.org/10.1007/s00382-016-3396-9

Maxwell, J. T., Harley, G. L., Mandra, T. E., Yi, K., Kannenberg, S. A., Au, T. F., Robeson, S. M., Pederson, N., Sauer, P. E., & Novick, K. A. (2019). Higher CO_2 concentrations and lower acidic deposition have not changed drought response in tree growth but do influence iWUE in hardwood trees in the Midwestern United States. *Journal of Geophysical Research: Biogeosciences*, *124*(12), 3798–3813.

Maxwell, J. T., Harley, G. L., Matheus, T. J., Strange, B. M., van Aken, K., Au, T. F., & Bregy, J. C. (2020). Sampling density and date along with species selection influence spatial representation of tree-ring reconstructions. *Climate of the Past*, *16*(5), 1901–1916. https://doi.org/10.5194/cp-16-1901-2020

Maxwell, J. T., Harley, G. L., & Robeson, S. M. (2016). On the declining relationship between tree growth and climate in the Midwest United States: The fading drought signal. *Climatic Change*, *138*, 127–142.

Maxwell, J. T., Harley, G. L., Tucker, C. S., Galuska, T., Ficklin, D. L., Bregy, J. C., Heeter, K. J., Au, T. F., Lockwood, B. R., King, D. J., & Maxwell, R. S. (2022). 1,100-year reconstruction of baseflow for the Santee River, South Carolina, USA reveals connection to the North Atlantic subtropical high. *Geophysical Research Letters*, *49*(22), e2022GL100742.

McDowell, N., Pockman, W. T., Allen, C. D., Breshears, D. D., Cobb, N., Kolb, T., Plaut, J., Sperry, J., West, A., Williams, D. G., & Yepez, E. A. (2008). Mechanisms of plant survival and mortality during drought: Why do some plants survive while others succumb to drought? *New Phytologist*, *178*(4), 719–739. https://doi.org/10.1111/j.1469-8137.2008.02436.x

McDowell, N. G., Allen, C. D., Anderson-Teixeira, K., Aukema, B. H., Bond-Lamberty, B., Chini, L., Clark, J. S., Dietze, M., Grossiord, C., Hanbury-Brown, A., Hurtt, G. C., Jackson, R. B., Johnson, D. J., Kueppers, L., Lichstein, J. W., Ogle, K., Poulter, B., Pugh, T. A. M., Seidl, R., … Xu, C. (2020). Pervasive shifts in forest dynamics in a changing world. *Science*, *368*(6494), eaaz9463. https://doi.org/10.1126/science.aaz9463

McDowell, N. G., Beerling, D. J., Breshears, D. D., Fisher, R. A., Raffa, K. F., & Stitt, M. (2011). The interdependence of mechanisms underlying climate-driven vegetation mortality. *Trends in Ecology & Evolution*, *26*(10), 523–532.

McEwan, R. W., Dyer, J. M., & Pederson, N. (2011). Multiple interacting ecosystem drivers: Toward an encompassing hypothesis of oak forest dynamics across eastern North America. *Ecography*, *34*(2), 244–256. https://doi.org/10.1111/j.1600-0587.2010.06390.x

Novick, K., Jo, I., D'Orangeville, L., Benson, M., Au, T. F., Barnes, M., Denham, S., Fei, S., Heilman, K., Hwang, T., Keyser, T., Maxwell, J., Miniat, C., McLachlan, J., Pederson, N., Wang, L., Wood, J. D., & Phillips, R. P. (2022). The drought response of eastern US oaks in the context of their declining abundance. *Bioscience*, *72*(4), 333–346. https://doi.org/10.1093/biosci/biab135

Novick, K. A., Ficklin, D. L., Grossiord, C., Konings, A. G., Martínez-Vilalta, J., Sadok, W., Trugman, A. T., Williams, A. P., Wright, A. J., Abatzoglou, J. T., Dannenberg, M. P., Gentine, P., Guan, K., Johnston, M. R., Lowman, L. E. L., Moore, D. J. P., & McDowell, N. G. (2024). The impacts of rising vapour pressure deficit in natural and managed ecosystems. *Plant, Cell & Environment*, 1–29. https://doi.org/10.1111/pce.14846

O'Neill, B. C., Tebaldi, C., van Vuuren, D. P., Eyring, V., Friedlingstein, P., Hurtt, G., Knutti, R., Kriegler, E., Lamarque, J.-F., Lowe, J., Meehl, G. A., Moss, R., Riahi, K., & Sanderson, B. M. (2016). The scenario model intercomparison project (ScenarioMIP) for CMIP6. *Geoscientific Model Development*, *9*(9), 3461–3482. https://doi.org/10.5194/gmd-9-3461-2016

Pan, Y., Chen, J. M., Birdsey, R., McCullough, K., He, L., & Deng, F. (2011). Age structure and disturbance legacy of North American

forests. *Biogeosciences*, *8*(3), 715–732. https://doi.org/10.5194/bg-8-715-2011

Pederson, N., Bell, A. R., Cook, E. R., Lall, U., Devineni, N., Seager, R., Eggleston, K., & Vranes, K. P. (2013). Is an epic pluvial masking the water insecurity of the greater New York City region? *Journal of Climate*, *26*(4), 1339–1354. https://doi.org/10.1175/JCLI-D-11-00723.1

Pederson, N. A. (2005). *Climatic sensitivity and growth of southern temperate trees in the eastern United States: Implications for the carbon cycle* [Ph.D., Columbia University]. Retrieved March 13, 2024, from http://www.proquest.com/docview/305015289/abstract/4BB17745306E4C38PQ/1

Robeson, S. M., Maxwell, J. T., & Ficklin, D. L. (2020). Bias correction of paleoclimatic reconstructions: A new look at 1,200+ years of Upper Colorado River flow. *Geophysical Research Letters*, *47*(1), e2019GL086689. https://doi.org/10.1029/2019GL086689

Rollinson, C. R., Alexander, M. R., Dye, A. W., Moore, D. J. P., Pederson, N., & Trouet, V. (2021). Climate sensitivity of understory trees differs from overstory trees in temperate mesic forests. *Ecology*, *102*(3), e03264. https://doi.org/10.1002/ecy.3264

Roman, D. T., Novick, K. A., Brzostek, E. R., Dragoni, D., Rahman, F., & Phillips, R. P. (2015). The role of isohydric and anisohydric species in determining ecosystem-scale response to severe drought. *Oecologia*, *179*(3), 641–654. https://doi.org/10.1007/s00442-015-3380-9

Schwarz, J., Skiadaresis, G., Kohler, M., Kunz, J., Schnabel, F., Vitali, V., & Bauhus, J. (2020). Quantifying growth responses of trees to drought—A critique of commonly used resilience indices and recommendations for future studies. *Current Forestry Reports*, *6*(3), 185–200. https://doi.org/10.1007/s40725-020-00119-2

Srivastava, A., Grotjahn, R., & Ullrich, P. A. (2020). Evaluation of historical CMIP6 model simulations of extreme precipitation over contiguous US regions. *Weather and Climate Extremes*, *29*, 100268.

Vicente-Serrano, S. M., Beguería, S., & López-Moreno, J. I. (2010). A multiscalar drought index sensitive to global warming: The standardized precipitation evapotranspiration index. *Journal of Climate*, *23*(7), 1696–1718. https://doi.org/10.1175/2009JCLI2909.1

Wehner, M. F., Arnold, J. R., Knutson, T., Kunkel, K. E., & LeGrande, A. N. (2017). *Chapter 8: Droughts, floods, and wildfires*. U.S. Global Change Research Program. https://doi.org/10.7930/J0CJ8BNN

Williams, A. P., Allen, C. D., Macalady, A. K., Griffin, D., Woodhouse, C. A., Meko, D. M., Swetnam, T. W., Rauscher, S. A., Seager, R., Grissino-Mayer, H. D., Dean, J. S., Cook, E. R., Gangodagamage, C., Cai, M., & McDowell, N. G. (2013). Temperature as a potent driver of regional forest drought stress and tree mortality. *Nature Climate Change*, *3*(3), 292–297. https://doi.org/10.1038/nclimate1693

Yi, K., Maxwell, J. T., Wenzel, M. K., Roman, D. T., Sauer, P. E., Phillips, R. P., & Novick, K. A. (2019). Linking variation in intrinsic water-use efficiency to isohydricity: A comparison at multiple spatiotemporal scales. *New Phytologist*, *221*(1), 195–208. https://doi.org/10.1111/nph.15384

Yu, S., Alapaty, K., Mathur, R., Pleim, J., Zhang, Y., Nolte, C., Eder, B., Foley, K., & Nagashima, T. (2014). Attribution of the United States "warming hole": Aerosol indirect effect and precipitable water vapor. *Scientific Reports*, *4*(1), 6929.

DATA SOURCES

Bi, D., Dix, M., Marsland, S., O'Farrell, S., Sullivan, A., Bodman, R., et al. (2020). Configuration and spin-up of ACCESS-CM2, the new generation Australian community climate and earth system simulator coupled model. *Journal of Southern Hemisphere Earth Systems Science*, *70*(1), 225–251.

Boucher, O., Denvil, S., Caubel, A., & Foujols, M. A. (2018). *IPSL IPSL-CM6A-LR model output prepared for CMIP6 CMIP*. https://doi.org/10.22033/ESGF/CMIP6.1534

Krasting, J. P., John, J. G., Blanton, C., McHugh, C., Nikonov, S., Radhakrishnan, A., Krasting, J. P., John, J. G., Blanton, C., McHugh, C., Nikonov, S., Radhakrishnan, A., Rand, K., Zadeh, N. T., Balaji, V., Durachta, J., Dupuis, C., Menzel, R., Robinson, T., … Zhao, M. (2018). *NOAA-GFDL GFDL-ESM4 model output prepared for CMIP6 CMIP historical*. https://doi.org/10.22033/ESGF/CMIP6.8597

Mauritsen, T., Bader, J., Becker, T., Behrens, J., Bittner, M., Brokopf, R., Brovkin, V., Claussen, M., Crueger, T., Esch, M., Fast, I., Fiedler, S., Fläschner, D., Gayler, V., Giorgetta, M., Goll, D. S., Haak, H., Hagemann, S., Hedemann, C., … Roeckner, E. (2019). Developments in the MPI-M Earth System Model version 1.2 (MPI-ESM1.2) and its response to increasing CO_2. *Journal of Advances in Modeling Earth Systems*, *11*(4), 998–1038.

Müller, W. A., Jungclaus, J. H., Mauritsen, T., Baehr, J., Bittner, M., Budich, R., Bunzel, F., Esch, M., Ghosh, R., Haak, H., Ilyina, T., Kleine, T., Kornblueh, L., Li, H., Modali, K., Notz, D., Pohlmann, H., Roeckner, E., Stemmler, I., … Marotzke, J. (2018). A higher-resolution version of the Max Planck Institute Earth System Model (MPI-ESM1.2-HR). *Journal of Advances in Modeling Earth Systems*, *10*(7), 1383–1413.

Swart, N. C., Cole, J. N. S., Kharin, V. V., Lazare, M., Scinocca, J. F., Gillett, N. P., Anstey, J., Arora, V., Christian, J. R., Hanna, S., Jiao, Y., Lee, W. G., Majaess, F., Saenko, O. A., Seiler, C., Seinen, C., Shao, A., Sigmond, M., Solheim, L., … Winter, B. (2019). The Canadian Earth System Model version 5 (CanESM5.0.3). *Geoscientific Model Development*, *12*(11), 4823–4873.

Tatebe, H., & Watanabe, M. (2018). *MIROC MIROC6 model output prepared for CMIP6 CMIP*. https://doi.org/10.22033/ESGF/CMIP6.881

Volodin, E., & Gritsun, A. (2018). Simulation of observed climate changes in 1850–2014 with climate model INM-CM5. *Earth System Dynamics*, *9*(4), 1235–1242.

Volodin, E. M., Mortikov, E. V., Kostrykin, S. V., Galin, V. Y., Lykossov, V. N., Gritsun, A. S., Diansky, N. A., Gusev, A. V., Iakovlev, N. G., Shestakova, A. A., & Emelina, S. V. (2018). Simulation of the modern climate using the INM-CM48 climate model. *Russian Journal of Numerical Analysis and Mathematical Modelling*, *33*(6), 367–374.

Wu, T., Lu, Y., Fang, Y., Xin, X., Li, L., Li, W., Jie, W., Zhang, J., Liu, Y., Zhang, L., Zhang, F., Zhang, Y., Wu, F., Li, J., Chu, M., Wang, Z., Shi, X., Liu, X., Wei, M., … Liu, X. (2019). The Beijing Climate Center Climate System Model (BCC-CSM): The main progress from CMIP5 to CMIP6. *Geoscientific Model Development*, *12*(4), 1573–1600.

Yukimoto, S., Kawai, H., Koshiro, T., Oshima, N., Yoshida, K., Urakawa, S., et al. (2019). The Meteorological Research Institute Earth System Model Version 2.0, MRI-ESM2.0: Description and basic evaluation of the physical component. *Journal of the Meteorological Society of Japan Series II*, *97*(5), 931–965.

Ziehn, T., Chamberlain, M. A., Law, R. M., Lenton, A., Bodman, R. W., & Dix, M. (2020). The Australian Earth System Model: ACCESS-ESM1.5. *Journal of Southern Hemisphere Earth Systems Science*, *70*(1), 193–214.

SUPPORTING INFORMATION

Additional supporting information can be found online in the Supporting Information section at the end of this article.

How to cite this article: Maxwell, J. T., Au, T. F., Kannenberg, S. A., Harley, G. L., Dannenberg, M. P., Ficklin, D. L., Robeson, S. M., Férriz, M., Benson, M. C., Lockwood, B. R., Novick, K. A., Phillips, R. P., Rochner, M. L., & Pederson, N. (2024). Asymmetric effects of hydroclimate extremes on eastern US tree growth: Implications on current demographic shifts and climate variability. *Global Change Biology*, *30*, e17474. https://doi.org/10.1111/gcb.17474